

Gate-Voltage Studies of Discrete Electronic States in Al Nanoparticles

D. C. Ralph^a, C. T. Black^b, and M. Tinkham

Department of Physics and Division of Engineering and Applied Science, Harvard University, Cambridge, MA 02138

We have investigated the spectrum of discrete electronic states in single, nm-scale Al particles incorporated into new tunneling *transistors*, complete with a gate electrode. The addition of the gate has allowed (a) measurements of the electronic spectra for different numbers of electrons in the *same* particle, (b) greatly improved resolution and qualitatively new results for spectra within superconducting particles, and (c) detailed studies of the gate-voltage dependence of the resonance level widths, which have directly demonstrated the effects of non-equilibrium excitations.

Recently it has become possible to measure the discrete spectrum of quantum energy levels for the interacting electrons within single semiconductor quantum dots [1] and nm-scale metal particles [2–4], and thereby to investigate the forces governing electronic structure. Our earlier experiments on Al particles were performed with simple tunneling devices, lacking a gate with which the electric potential of the particle could be adjusted. In this Letter, we describe the fabrication and study of nanoparticle *transistors*, complete with a gate electrode. This greatly expands the accessible physics. We have used the gate to tune the number of electrons in the particle, so as to measure excitation spectra for different numbers of electrons in the same grain and to confirm even-odd effects. The gate has also allowed significantly improved spectroscopic resolution, providing new understanding about the destruction of superconductivity in a nm-scale metal particle by an applied magnetic field. Studies of the gate-voltage dependence of tunneling resonance widths have shown that non-equilibrium excitations in the nanoparticle are a primary source of resonance broadening.

A schematic cross-section of our device geometry is shown in Fig. 1(a). The gate electrode forms a ring around the Al nanoparticle. The devices are fabricated by first using electron beam lithography and reactive ion etching to make a bowl-shaped hole in a suspended silicon nitride membrane, with an orifice between 5 and 10 nm in diameter [5]. The gate electrode is formed by evaporating 12 nm of Al onto the flat (lower in Fig. 1(a)) side of the membrane. Plasma anodization and deposition of insulating SiO₂ are then used to provide electrical isolation for the gate. We next form an aluminum electrode which fills the bowl-shaped side (top in Fig. 1(a)) of the nitride membrane by evaporation of 100 nm of Al, followed by oxidation in 50 mtorr O₂ for 45 sec to form a tunnel barrier near the lower opening of the bowl-shaped hole. We create a layer of nanoparticles by depositing 2.5 nm of Al onto the lower side of the device; due to surface tension the metal beads up into separate grains less than 10 nm in diameter [6]. In approximately 25%

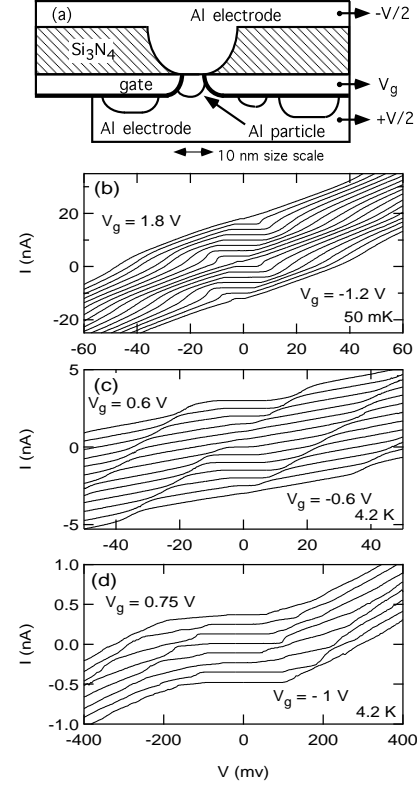


FIG. 1. (a) Schematic cross section of device geometry. (b)-(d) Current-voltage curves displaying Coulomb-staircase structure for three different samples, at equally spaced values of gate voltage. Data for different V_g are artificially offset on the current axis.

of the samples (determined as those showing “Coulomb-staircase” structure as described below), a single particle forms under the nm-scale tunnel junction to contact the top Al electrode. Finally, after a second oxidation step to form a tunnel junction on the exposed surface of the particle, a lower electrode is formed by evaporating 100 nm of Al to cover the particle. We measure electron tunneling between the top and bottom electrodes, through a single nanoparticle, as a function of gate voltage, V_g .

The devices can be characterized by measuring large-scale current vs. source-drain voltage (I - V) curves for a series of V_g (Fig. 1(b)-(d)). The form of these curves, with zero current at low $|V|$ (the “Coulomb blockade”), sloping steps equally spaced in V , and step thresholds sensitive to V_g , is indicative of single-electron tunneling via one nanoparticle [7]. From the positions of the voltage thresholds for steps in the I - V curve, we can determine

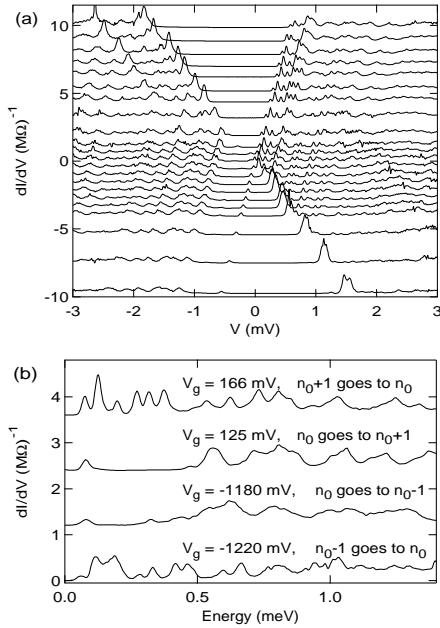


FIG. 2. (a) dI/dV vs. source-drain voltage, plotted for V_g ranging from 75 mV (bottom) to 205 mV (top), for the device of Fig. 1(b). Curves are offset on the dI/dV axis. (b) Tunneling spectra for this sample, labeled by the number of electrons in the initial and final states. (n_0 is odd) All data are for $T=50$ mK, $H=0.05$ Tesla, to drive the Al leads normal.

the capacitances within the device [8]. For Fig. 1(b), the lead-to-particle capacitances are $C_1 = 3.5$ aF and $C_2 = 9.4$ aF, and the gate-to-particle capacitance is $C_g = 0.09$ aF; for Fig. 1(c) the capacitances are 3.4, 8.5, and 0.23 aF, and for Fig. 1(d) 0.6, 1.0, and 0.13 aF. The charging energy, $E_c = e^2/(2C_{total})$, for these devices is relatively large – for the device of Fig. 1(d), $E_c = 46$ meV (corresponding to $T \sim 500$ K), comparable to the largest blockade energy measured for any single-electron transistor [9].

The nanoparticle size can be estimated using a value for the capacitance per unit area, 0.075 aF/nm², determined from larger tunnel junctions made using our oxidation process. If we make the crude assumption of a hemispherical particle shape, and base the estimate on the larger lead-to-particle capacitance, we estimate radii of 4.5, 4.3, and 1.5 nm, respectively, for Fig. 1(b)-(d).

To measure the discrete electronic states within the nanoparticle, we cool the devices to mK temperatures and measure dI/dV vs. V in the range of the first Coulomb-staircase step (Fig. 2(a)). Peaks in dI/dV are expected whenever the Fermi level in one of the two leads becomes equal to the threshold energy for an electron to tunnel either into or out of one of the discrete states within the particle, through one of the two tunnel junctions [10]. The interpretation that the data in Fig. 2(a) are due to tunneling via states in a single nanoparticle is

confirmed by the uniform shifting of the peaks with V_g . All the dI/dV peaks shift linearly in V as a function of V_g , with tunneling thresholds across junction 1 all moving with a single slope, $\Delta V \approx (C_g/C_2)\Delta V_g$, and thresholds across junction 2 moving as $\Delta V \approx (C_g/C_1)\Delta V_g$. Due to the large charging energy in this device, electrons must tunnel one at a time through the particle in the V range displayed in Fig. 2(a). This means that at fixed V_g all the peaks associated with the same junction are due to states with the *same* number of electrons.

As V_g is increased in Fig. 2(a), the extent of the Coulomb blockade region at low $|V|$ decreases, goes to 0, and then increases. This zero-crossing indicates that an electron is added to the particle. If n_0 is the number of electrons in the ground state at $V_g=V=0$, then the tunneling processes which overcome the Coulomb blockade correspond in the bottom half of Fig. 2(a) to $n_0 \rightarrow (n_0 + 1)$ -electron transitions, and in the top half of the figure to $(n_0 + 1) \rightarrow n_0$ transitions. The $n_0 \rightarrow (n_0 + 1)$ and $(n_0 + 1) \rightarrow n_0$ -electron spectra can be determined most easily from the lower left and upper right quadrants of Fig. 2(a), respectively. In these quadrants, the tunneling step which overcomes the Coulomb blockade occurs across the higher resistance junction [11], so that tunneling across this junction is always the rate-limiting step for current flow. All the peaks in dI/dV correspond to states which provide alternative tunneling channels across this one junction. In the other two quadrants, thresholds for tunneling across both tunnel junctions, *i.e.* for both $n_0 \rightarrow (n_0 + 1)$ and $(n_0 + 1) \rightarrow n_0$ processes, are visible.

In Fig. 2(b), we display several tunneling spectra for different numbers of electrons in the same particle. (We discuss the significance of these spectra below.) Fig. 3 shows the magnetic-field (H) dependence of the levels which can be resolved in the upper two curves of Fig. 2(b). In both Figs. 2(b) and 3, we have converted from source-drain bias to electron energy, multiplying by $eC_2/(C_1 + C_2) = 0.73e$ to account for the capacitive division of V across the two tunnel junctions. The values of V_g were chosen so that the spectra were measurable at low values of $|V|$, where they are best resolved. As a function of H , the energy levels are shifted approximately linearly, with Zeeman splittings corresponding to g values between 1.95 and 2. Energy levels which move to higher energies with increasing H produce broader, less distinct dI/dV peaks than downward-moving levels (for reasons poorly understood), and can be followed for only a limited range of H before they are lost in background. In our previous superconducting particles, without gates, most upward-moving levels could not be resolved at all. This caused us to incorrectly assign anomalously low g -factors to some states [3].

As described previously [2], the electron-number parity in the ground state of a particle can be determined by whether the lowest-energy tunneling level exhibits Zeeman splitting (even parity) or not (odd). In this way we can tell that n_0 is odd in Fig. 3(a) and $n_0 + 1$ is even in Fig. 3(b). While tuning V_g , we have observed parity

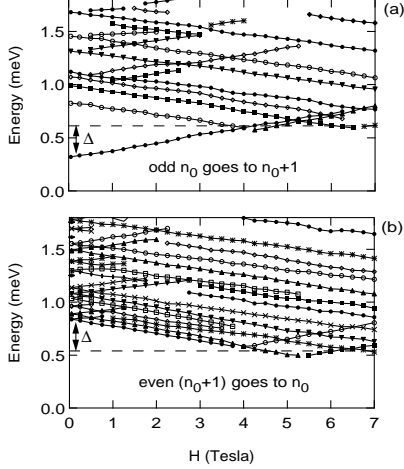


FIG. 3. Magnetic field dependence of the resolved electronic states for the device of Fig. 2 at (a) $V_g = 110$ mV and (b) $V_g = 181$ mV.

changes only when electrons are added to the particle at the zero-crossings of the Coulomb blockade. The parity simply switches from even to odd to even, etc., at consecutive blockade minima. The nanoparticle therefore exchanges electrons only with the electrodes, and not with any nearby defects.

The ability to tune the number of electrons in a particle using V_g allows us for the first time to study the dramatic differences between tunneling spectra for even and odd numbers of electrons in the *same* superconducting particle [3]. The large gap between the lowest energy level and all the others in the $n_0 \rightarrow n_0 + 1$ and $n_0 \rightarrow n_0 - 1$ spectra (Figs. 3(a) and 2(b)) can be explained by superconducting pairing. The tunneling states in these spectra have an even number of electrons, so that the lowest level is the fully paired superconducting state. Tunneling via any other state requires the production of at least two quasiparticles, with a large extra energy cost approximately twice the superconducting gap, Δ . The $n_0 + 1 \rightarrow n_0$ and $n_0 - 1 \rightarrow n_0$ tunneling states have an odd number of electrons, and they all must contain at least one quasiparticle. Hence there is no large gap within these spectra. However, the contribution of Δ to the quasiparticle energy causes the low-lying tunneling levels at low H to have energies greater by Δ than at large H , where superconductivity is suppressed. The first tunneling thresholds in Fig. 3(a) and (b) have exactly the same H dependence, with opposite sign, because they correspond to the filling and emptying of the same quantum states. In Fig. 3, $\Delta \approx 0.3$ meV, comparable to previous results [3].

The levels in Figs. 3(a,b) provide new insights as to how a magnetic field destroys superconductivity in a nanoparticle. Consider the second level at small H in Fig. 3(a), which begins near 0.8 meV. This state shifts

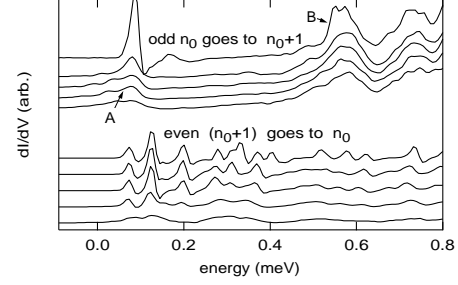


FIG. 4. Tunneling resonances broaden and develop substructure as V_g is used to shift them to larger values of $|V|$. The top scan in both sets corresponds to a value of V_g which allows the spectrum to be measured with minimum $|V|$. Going down, other scans are for V_g requiring extra source-drain voltages $\delta|V| = 0.2, 0.4, 0.6$, and 1.2 mV. The scans are artificially shifted in energy to align peaks due to the same eigenstates. $T=50$ mK, $H=0$ for all scans, and the sample is the same as in Figs. 2 and 3. Peaks A and B are discussed in the text.

down as a function of H , due to its spin-1/2 Zeeman energy, up to ~ 4 Tesla. There it disappears in favor of a new upward-moving (opposite spin-1/2) level. This means that the originally-empty downward-trending level drops below the energy of an originally-filled upward-trending level, and an electron is transferred between the states. The odd-electron ground state changes its spin from 1/2 to 3/2 \hbar . As this process is repeated, the tunneling threshold moves in a continuous zig-zag pattern, and the ground state successively increases its spin in units of \hbar . A similar argument for Fig. 3(b) shows that the even-electron ground state also evolves by individual spin flips. Superconductivity is destroyed as electrons flip one at a time. In contrast, the classic theories of Clogston and Chandrasekhar [12], for a superconducting transition driven by spin pair-breaking, predict a large discontinuous jump in the tunneling threshold, at a field where many spins flip simultaneously. Investigations are underway as to whether these theories do not properly take into account the effect of discrete electronic energy levels in the particle [13], or perhaps whether the experimental transitions are made continuous by a contribution from orbital pair breaking [14].

We have shown that changes in V_g act to shift the electrostatic energy of the eigenstates on the nanoparticle, and thereby shift the value of V at which a given state produces a peak in dI/dV (see Fig. 2(a)). In Fig. 4, we examine more closely how the *shapes* of resonances change as they are moved to larger values of $|V|$. The top spectrum in each set of traces corresponds to a value of V_g which places the first tunneling peak at the smallest possible $|V|$ [15]. The lower curves show the results of tunneling via the same quantum states, after their dI/dV peaks have been shifted to successively larger $|V|$. To aid comparison, we have aligned the spectra, so that the shifts

in $|V|$ are not displayed explicitly. We show data for superconducting electrodes ($H=0$) because the BCS singularity in the density of states in the electrodes improves spectroscopic resolution [2]. Focus first on the lowest energy level for $n_0 \rightarrow n_0 + 1$ (odd-to-even) electron tunneling. In equilibrium, this is necessarily a single, non-degenerate state – the fully-paired superconducting state. Indeed, for the lowest- $|V|$ trace (top curve), this level produces a single sharp signal (whose shape is given by the derivative of the BCS density of states in the Al electrode [2]). However, as V_g is used to shift this first state to larger $|V|$, the resonance quickly broadens and develops substructure. The substructure cannot be explained by heating in the electrodes. Instead, it is evidence for the importance of non-equilibrium excitations *within* the particle [4]. When electrons are tunneling via even the lowest level in the $n_0 \rightarrow n_0 + 1$ spectrum, the current flow will naturally generate non-equilibrium excitations within the particle when the excess source-drain energy, $e(\delta|V|)$, is greater than the difference between the first two levels in the measured $n_0 + 1 \rightarrow n_0$ spectrum (~ 0.05 meV). This happens because one electron can tunnel from the high-energy electrode into the empty level in the particle, and then an electron can exit to the other electrode from a *different*, lower-energy ($n_0 + 1$)-electron filled state, leaving a hole. If the resultant electron-hole excitation does not relax before the next electron tunnels onto the particle ($e/I \sim 10^{-8}$ s), its presence can produce small shifts in the tunneling energies available for the next electron. For very small particles, it has been proposed that the time-integrated result for an ensemble of possible excitations will be a well-resolved cluster of tunneling resonances associated with each single-electron level [4]. For particles large enough to exhibit superconductivity, we propose that the different non-equilibrium resonances are not so well resolved, but overlap to produce broadened dI/dV peaks.

In sharp contrast to the $n_0 \rightarrow n_0 + 1$ spectrum, the low-energy peaks in the $n_0 + 1 \rightarrow n_0$ spectrum do not show increasing widths as long as $\delta|V| \leq 0.6$ meV, but then they do broaden for larger $\delta|V|$. This is additional evidence for the role of non-equilibrium excitations in resonance broadening, because the condition necessary for producing non-equilibrium excitations in the particle during measurement of these $n_0 + 1 \rightarrow n_0$ states is that $e(\delta|V|)$ must be greater than the difference between the first two levels in the $n_0 \rightarrow n_0 + 1$ spectrum (~ 0.55 meV).

In the raw data, the first peak (A) in the $\delta|V| = 0.6$ mV scan of the $n_0 \rightarrow n_0 + 1$ spectrum in Fig. 4 and the second peak (B) in the $\delta|V| = 0$ scan of the same spectrum occur at the same value of V , so the degree of non-equilibrium in the particle should be similar. The effective widths of these dI/dV peaks are nearly the same. This suggests that the non-equilibrium effect is also a dominant source of broadening for the higher-energy resonances, even in the $\delta|V| = 0$ spectrum.

In summary, we have produced tunneling transistors

containing single Al nanoparticles, and have measured the discrete spectra of energy levels in the particle while tuning the number of electrons it contains. We have directly demonstrated differences in level spectra for even vs. odd numbers of electrons, which can be explained as an effect of superconducting pairing interactions. The application of a magnetic field destroys superconductivity in the nanoparticle by a sequence of individual spin flips. The tunneling resonances broaden and develop substructure when the source-drain voltage becomes large enough to allow the production of non-equilibrium excitations within the particle.

We thank F. Braun and J. von Delft for discussions, and R. C. Tiberio for help in device fabrication. This research was supported by NSF Grant No. DMR-92-07956, ONR Grant No. N00014-96-1-0108, JSEP Grant No. N00014-89-J-1023, and ONR AASERT Grant No. N00014-94-1-0808, and was performed in part at the Cornell Nanofabrication Facility, funded by the NSF (Grant No. ECS-9319005), Cornell University, and industrial affiliates.

-
- ^a Present address: Physics Department, Cornell University, Ithaca, NY 14853.
- ^b Present address: IBM T. J. Watson Research Center, Yorktown Heights, NY 10598.
- [1] For reviews, see M. A. Kastner, *Physics Today* **46** No. 1, 24 (1993); R. C. Ashoori, *Nature* **379**, 413 (1996).
 - [2] D. C. Ralph, C. T. Black, and M. Tinkham, *Phys. Rev. Lett.* **74**, 3241 (1995).
 - [3] C. T. Black, D. C. Ralph, and M. Tinkham, *Phys. Rev. Lett.* **76**, 688 (1996).
 - [4] O. Agam *et al.*, cond-mat/9611115.
 - [5] K. S. Ralls, R. A. Buhrman, and R. C. Tiberio, *Appl. Phys. Lett.* **55**, 2459 (1989).
 - [6] H. R. Zeller and I. Giaever, *Phys. Rev.* **181**, 789 (1969).
 - [7] For a review, see *Single Charge Tunneling*, ed. H. Grabert and M. H. Devoret (Plenum Press, NY, 1992).
 - [8] A. E. Hanna and M. Tinkham, *Phys. Rev. B* **44**, 5919 (1991).
 - [9] Y. Takahashi *et al.*, *Electron Lett.* **31**, 136 (1995); E. Leobandung *et al.*, *Appl. Phys. Lett.* **67**, 938 (1995); Y. Nakamura, D. L. Klein, and J. S. Tsai, *Appl. Phys. Lett.* **68**, 275 (1996); P. L. McEuen *et al.*, reported at the NATO ASI conference on Mesoscopic Physics (1996).
 - [10] D. V. Averin and A. N. Korotkov, *J. Low Temp. Phys.* **80**, 173 (1990).
 - [11] From fits to Fig. 1(b), the 3.5 aF tunnel junction has a resistance of approximately 2 M Ω , and the 9.4 aF junction 200 k Ω .
 - [12] A. M. Clogston, *Phys. Rev. Lett.* **9**, 266 (1962); B. S. Chandrasekhar, *Appl. Phys. Lett.* **1**, 7 (1962).
 - [13] F. Braun and J. von Delft, personal communication.
 - [14] R. Meservey and P. M. Tedrow, *Physics Reports* **238**, 173 (1994); P. Fulde, *Adv. in Physics* **22**, 667 (1973).
 - [15] With superconducting electrodes, $e|V| \geq$ twice the gap in the electrodes is necessary to initiate tunneling.